Self-Assembly of Hydrogensquarates: Crystal Structures and Properties

B. B. Koleva,*,† T. Kolev,‡ R. W. Seidel,† M. Spiteller,‡ H. Mayer-Figge,† and W. S. Sheldrick†

Lehrstuhl für Analytische Chemie, Ruhr-Universität Bochum, Universitätsstraβe 150, 44780 Bochum, Germany, and Institut für Umweltforschung, Universität Dortmund, Otto-Hahn-Strasse 6, 44221 Dortmund, Germany

Received: December 3, 2008; Revised Manuscript Received: January 12, 2009

The self-assembly of the hydrogensquarates is elucidated by means of linear-polarized infrared (IR-LD) spectroscopy of oriented colloids in nematic host and the so-called reducing-difference procedure for polarized IR-LD spectra interpretation. The scopes and limitation are discussed on five novel derivatives of squaric acid and its anions, that is, 2-chloro-3-aminopyridinium hydrogensquarate (**1**), bis (1,2,3,4-tetrahydroquinolinium) squarate (**2**), bis hydrogensquarate dihydrate salt of 4-(aminomethyl)pyridine (**3**), *N*-(2-ammoniumethyl)-piperazinium monohydrate hydrogensquarate squarate (**4**), and 3-nitropyridinium hydrogensquarate monohydrate (**5**), respectively. The structures of these compounds **1**−**5** were solved by means of single-crystal X-ray diffraction, and the crystallographic data were used for the experimental elucidation of the corresponding IR spectra of crystals with respect to studying Fermi-resonance (FR), Davydov splitting (DS), and Fermi−Davydov (FD) as well as Evans' hole effects. The various motifs for self-assembly of squaric acid and its anions in the organic crystals are discussed together with their IR-spectroscopic properties.

Introduction

The investigation of the vibrational spectra and in particular IR spectra of hydrogen-bonded systems in the solid state is an important topic in physics, chemistry, and biology. However, these spectra are as a rule complicated as a result of significant anharmonic effects of the high frequency intermolecular vibrations in crystals. Two aspects complicate this problem. The first of these is Fermi-resonance (FR), which occurs between a fundamental vibration and a combination (or overtone) of the molecule. The second is splitting that arises from intermolecular interaction and transmission of vibrational excitation from one molecule to another in a crystal. As a result, one nondegenerate vibration of the free molecule may be split in the crystal into a multiplet of bands.[1,2] The number of components is equal to the number of molecules in the crystal unit cell, and the polarization of these bands can be different (the effect was named[3,4] as Davydov splitting (DS)). The problem of combined Fermi−Davydov (FD) resonance in crystals was considered by Lisitsa et al.[5−9]

However, in all of the above-mentioned fundamental research, it has been demonstrated that the components of the multicomponent spectroscopic patterns have different polarizations, depending on the origin. For these reasons, the possibilities of the linear-polarized infrared (IR-LD) spectroscopy can be used for experimental assignment of the phenomena in crystalline compounds. In this respect, we have been using an orientation method involving colloid suspensions in a nematic liquid crystal host in our research. This method was employed for the first time in 2004 by Ivanova at al. (see refs 30, 31) as a tool for the partial orientation of solids, to be examined by IR-LD spectroscopy. It has been found that it is possible to perform spectroscopic and structural elucidation of the embedded compounds, independently of their melting point, crystalline or amorphous state, and the quality of the single crystals or polycrystalline samples. Our investigations demonstrate that the method permits the study of inorganic and organic compounds, metal complexes, and glasses. With our current research, we have been able to demonstrate the excellent potential of this tool for the investigation of crystalline samples using five newly synthesized and structurally characterized model compounds, 2-chloro-3-aminopyridinium hydrogensquarate (**1**), bis (1,2,3,4-tetrahydroquinolinium) squarate (**2**), bis hydrogensquarate dihydrate salt of (4-pyridylmethyl)amine (**3**), *N*-(2-ammoniumethyl)-piperazinium monohydrat hydrogensquarate squarate (**4**), and 3-nitropyridinium hydrogensquarate monohydrate (**5**) (Scheme S1). All of these compounds are derivatives of squaric acid and its anions, which have been systematically studied by us with respect to designing new materials with second-order nonlinear optical (NLO) properties. Squaric acid (H_2Sq) provides an attractive template for generating tightly hydrogen-bonded self-assemblies from polarizable cations in general and leads to the isolation of new materials with NLO properties in the bulk. The presence of H_2Sq and its anions in the solid state leads to the possibility of controlling the assembly of individual molecules in solids, using hydrogen bonding as a powerful noncovalent force for organizing organic molecules.[10−24]

The following self-assembly patterns of squaric acid itself and its anions HSq^- and Sq^{2-} have been identified up to now in crystal structures (Scheme 1): (HSq^-) individual α-dimers (**Ia**) and two independent isolated α-dimers (**Ib**), HSq^- α-chains (**IIa**, **IIb**), and HSq^- *β*-chains (**IIIa**, **IIIb**), differing by the disposition of the anion with respect to the chain. In **IIIa**, all of the HSq^- are coplanar, while in **IIIb**, they are orientated in a mutually perpendicular mannner. In the tetrameric structural motifs (**IVa**, **IVb**, **IVc**), we can distinguish three known fragments, **IVa** with equivalent HSq^- anions disposed in a planar manner, **IVb** with equivalent HSq^- anions that are orientated in mutually perpendicular pairs, and the tetrameric motif $H_2Sq\cdot 2HSq^-\cdot Sq^{2-}$ (**IVc**) consisting of different forms of squaric acid. Other motifs include $H_2Sq\cdot HSq^-$ double *β*-chains (**V**) and chains of α-dimers (**VI**), isolated (Sq^{2-}) dianions (**VII**), isolated hydrogensquarate anions (**VIII**), as well

* Corresponding author. Tel.: (0234 32-24190). E-mail: bkoleva@chem.uni-sofia.bg.
† Ruhr-Universität Bochum.
‡ Universität Dortmund.

10.1021/jp8106233 CCC: $40.75
Published on Web 03/11/2009

SCHEME 1: Structural Motifs of H_2Sq and Its HSq^- and Sq^{2-} Ions[a]

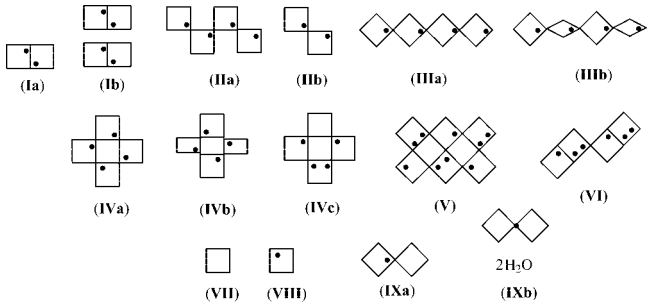

[a] The squaric acid fragments are represented as a square, and the hydroxyl positions are represented by dots.[25]

as fragments with $HSq^- \cdot Sq^{2-}$ moieties exhibiting a pseudo b-type of interaction (**IXa**) and with averaged disposition of the hydrogen atom between both the anion moieties and the included solvent molecules (**IXb**). It is reasonable to expect that a further systematic variation of the counterion in salts of the HSq^- and/or Sq^{2-} anions should lead to the isolation of additional novel self-assembly motifs and that these could exhibit interesting optical and/or nonlinear optical properties. Compounds with motif **IXb** are characterized by their red color in the solid state, which is associated with this unique type of self-organization of the anions in the crystals.[10] A further example in this respect is the novel compound **5**, reported here. The important aspect in the context of our investigation is that these systems were fully characterized by IR spectroscopy, where we can observe all of the discussed above phenomena as well as the Evans' hole effect.

Experimental Section

Materials and Methods. The X-ray diffraction intensities were measured on an Oxford Diffraction XCalibur2 diffractometer with Sapphire2 CCD for **1** and on a Siemens P4 four-circle diffractometer for **2**−**5**, always using graphite monochromatized Mo Kα radiation and employing the ω scan mode. The data were corrected for Lorentz and polarization effects. An absorption correction based on multiple scanned reflections[26] was applied to the data of **1**, and a psi-scan correction was performed for the data of **4** with ABSPsiScan from the Platon program.[26] The crystal structures were solved by direct methods using SHELXS-97[27] with the exception of **5**. This was solved ab initio by charge flipping with the flipper routine of the Platon program. The crystal structures were refined by full-matrix least-squares refinement against F^2.[27] Anisotropic displacement parameters were introduced for all non-hydrogen atoms with the exception of **4**. In the structure of **4**, only oxygen atoms were refined anisotropically with respect to the data/parameter ratio. Because of the absence of anomalous scattering, Friedel opposites were merged during the refinement of **4**, and the absolute configuration was assigned arbitrarily. The hydrogen atoms attached to carbon were placed at calculated positions and refined, allowing them to ride on the parent carbon atom. The hydrogen atoms bound to nitrogen and the oxygen were constrained to the positions that were confirmed from the difference map and refined with the appropriate riding model, with the exception of the amino and water hydrogen atoms. The hydrogen atoms of the amino group in **1** and the water molecules in **3** and **5** were located from the difference map and refined with fixed N−H and O−H distances of 0.88(2) and 0.82(2) Å, respectively. The water hydrogen atoms of **4** could not be located in the final difference synthesis and were therefore excluded from the refinement. Relevant crystallographic structure data and refinement details are presented in Table 1, and selected bond distances and angles are in Table S1.

The IR spectra were measured on a Thermo Nicolet 6700 FTIR spectrometer (4000−400 cm^{-1}, 2 cm^{-1} resolution, 200 scans) equipped with a Specac wire-grid polarizer. Nonpolarized solid-state IR spectra were recorded using the KBr disk technique. The oriented samples were obtained as a suspension in a nematic liquid crystal (ZLI 1695 and MLC 6815, Merck). The theoretical approach and the experimental technique for preparing the samples, as well as procedures for polarized IR-spectra interpretation and the validation of this new linear-dichroic infrared (IR-LD) orientation solid-state method for accuracy, precision, and the influence of the liquid crystal medium on peak positions and integral absorbances of the guest molecule bands, have been presented previously.[28−31] Spectroscopic and structural results obtained by the presented orientation technique were obtained using the known reducing-difference procedure designated as "stepwise reduction" for polarized IR-spectra interpretation.[28−31] The Fermi-resonance effect is proved independently by the obtained deuterated analogues of the studied system.

The analyses of the samples by HPLC-ESI MS/MS were performed with a Thermo Finnigan surveyor LC-pump. Compounds were separated on a Luna C18 column (150 × 2 mm, 4 μm particle size) from Phenomenex (Torrance, CA). The mobile phase consisted of water + 0.1% HCOOH (A) and acetonitrile + 0.1% HCOOH (B) using a gradient program presented in Table S2.

The elemental analysis was carried out according to the standard procedures for C and H (as CO_2 and H_2O) and N (by the Dumas method). The thermogravimetric study was carried out using a Perkin-Elmer TGS2 instrument. The calorimetric measurements were performed on a DSC-2C Perkin-Elmer apparatus under argon.

Synthesis. The starting compounds for the synthesis of **1**, 2-chloro-3-aminopyridine, and squaric acid (H_2Sq) were products of Merck (Germany). 0.128 g of 2-chloro-3-aminopyridine and 0.114 g of H_2Sq were dissolved in 25 mL of aqueous solution, and the solution was stirred for 24 h at 40 °C. The resulting yellow crystals were filtered off, washed with C_2H_5OH, and dried on P_2O_5 at 298 K. Yield 88%. Anal. Calcd for $C_9H_7O_4N_3Cl$: C, 42.12; H, 2.75; N, 16.37. Found: C, 42.10; H, 2.73; N, 16.35. The most intensive signal in the mass spectra of **1** is the peak at *m*/*z* 129.52, corresponding to the singly charged $[C_5H_6N_2Cl]^+$ ion with an *m*/*z* value of 129.57. The thermal methods within the range 300−500 K indicate an absence of the included solvent molecules. Compound **2** is obtained in the same way as **1**, by mixing equimolar amounts of 1,2,3,4-tetrahydroquinoline (0.133 g) and H_2Sq (0.114 g). However, in this case, the resulting colorless crystals correspond to the compound bis (1,2,3,4-tetrahydroquinolinium) squarate (**2**). Yield 92%. Anal. Calcd for $C_{22}H_{24}O_4N_2$: C, 69.46; H, 6.36; N, 7.36. Found: C, 69.48; H, 6.35; N, 7.35. The most intensive signal in the mass spectra of **2** is the peak at *m*/*z* 134.59, corresponding to the singly charged $[C_9H_{12}N]^+$ ion with an *m*/*z* value of 134.20. Similar to **1**, compound **2** does not contain solvent molecules, on the basis of the applied thermal methods. Compound **3**, the bis hydrogensquarate dihydrate salt of (4-pyridylmethyl)amine, was synthesized using the common synthetic scheme described above by mixing 0.108 g of the (4-pyridylmethyl)amine with 0.228 g of squaric acid, preliminary dissolved in 25 mL of aqueous solution. Yield 90%. Anal. Calcd

TABLE 1: Crystallographic and Refinement Data for 1−5

	1	2	3	4	5
empirical formula	$C_9H_7ClN_2O_4$	$C_{22}H_{24}N_2O_4$	$C_{14}H_{12}N_2O_8 \cdot 2H_2O$	$C_{14}H_{19}N_3O_8 \cdot H_2O$	$C_9H_6N_2O_6 \cdot H_2O$
M_r	242.62	380.43	372.29	375.34	256.17
crystal size	0.27 × 0.17 × 0.05	0.35 × 0.21 × 0.15	0.20 × 0.15 × 0.13	0.59 × 0.54 × 0.42	crystal size
crystal system	triclinic	triclinic	monoclinic	monoclinic	monoclinic
space group	$P\bar{1}$	$P\bar{1}$	$P2/c$	$P2_1$	$C2/c$
T [K]	108(2)	294(2)	294(2)	294(2)	294(2)
λ [Å]	0.71073	0.71073	0.71073	0.71073	0.71073
a [Å]	7.085(1)	7.535(2)	15.438(2)	7.670(2)	20.649(8)
b [Å]	7.229(1)	8.023(2)	8.0515(8)	11.670(2)	8.035(2)
c [Å]	9.527(2)	8.827(2)	13.162(1)	9.440(2)	12.977(5)
α [deg]	93.47(1)	89.54(3)	90	90	90
β [deg]	91.03(1)	77.42(3)	100.579(6)	105.48(3)	97.38(3)
γ [deg]	99.86(1)	66.86(3)	90	90	90
V [Å]	479.6(1)	477.1(2)	1608.2(3)	814.3(3)	2135(1)
Z	2	1	4	2	8
μ [mm^{-1}]	0.398	0.092	0.133	0.129	0.141
ρ_{calc} [mg m^{-3}]	1.680	1.324	1.538	1.531	1.594
2θ [deg]	50.00	50.00	50.00	50.10	50.20
reflections collected	2207	1815	3697	1623	1947
unique reflections	1597	1678	2819	1518	1894
R_{int}	0.036	0.019	0.029	0.072	0.030
observed reflections [$I > 2\sigma(I)$]	1053	1229	1998	833	1211
GOF on F^2	0.859	1.035	1.020	1.078	1.009
R_1 [$I > 2\sigma(I)$]	0.042	0.043	0.045	0.071	0.041
wR_2 (all data)	0.076	0.118	0.115	0.160	0.109
residuals [e Å^{-3}]	0.27/−0.26	0.19/−0.17	0.16/−0.23	0.27/−0.33	0.20/−0.17

for $C_{14}H_{16}O_{10}N_2$: C, 45.17; H, 4.33; N, 7.52. Found: C, 45.15; H, 4.33; N, 7.53. The thermal methods within the range 300−500 K indicate a weight loss of 9.67% and an enthalpy effect of 16.23 kcal/mol at 127 °C, corresponding to the presence of two solvent molecules in the crystal lattice of **3**. The crystals of *N*-(2-ammoniumethyl)-piperazinium monohydrate hydrogensquarate squarate (**4**) were obtained by the reaction of the *N*-(2-ammoniumethyl)-piperazine (0.128 g) with H_2Sq (0.228 g) dissolved in 50 mL of water. Yield 72%. Anal. Calcd for $C_{14}H_{20}O_9N_3$: C, 44.92; H, 5.39; N, 11.23. Found: C, 44.91; H, 5.40; N, 11.25. The thermal methods within the range 300−500 K indicate a weight loss of 4.80% and an enthalpy effect of 7.12 kcal/mol at 125 °C, corresponding to one solvent molecule being included in the crystal lattice of **4**. When 0.124 g of 3-nitropyridine was mixed with 0.114 g of H_2Sq in 25 mL of water, the resulting red ($\lambda_{max} = 512$ nm) crystals (yield of 91%) for component **5**, 3-nitropyridinum hydrogensquarate monohydrate $C_9H_8O_7N_2$, give the following values. Anal. Calcd: C, 42.20; H, 3.15; N, 10.94. Found: C, 42.18; H, 3.15; N, 10.95. The thermal methods within the range 300−500 K exhibit a weight loss of 7.15% and an enthalpy effect of 7.15 kcal/mol at 138 °C, corresponding to a solvent molecule being included in the crystal lattice of **5**. The observed higher temperature value for the loss of the solvent molecule being can be assigned to the presence of a stronger interaction in the crystal structure involving the participation of the solvent molecules.

Results and Discussion

Crystal Structures of 1−5. The compound 2-chloro-3-aminopyridinium hydrogensquarate (**1**) crystallizes in the triclinic space group $P\bar{1}$. An ORTEP diagram is given in Figure 1. All molecular geometry parameters exhibit typical values. The hydrogensquarate ions form a classical stable α-dimer (**Ia** in Scheme 1) via interanion hydrogen-bonding interactions. The observed O−H···O distance in this structural motif (2.544(3) Å) indicates a moderately strong hydrogen bond and correlates well with the data of other dimers of this type.[17] The cations and anions are joined by N−H···O hydrogen bonds via the pyridinium moiety and the amino group (Figure 2). The N−H···O distances are with lengths corresponding to moderate (2.613(3) and 2.924(3) Å) as well as weak (3.193(3) Å) interactions, respectively. This leads to 2D infinite layers with an interlayer distance of about 3 Å. The reported structure of **1** is the second crystallographically characterized salt of 2-chloro-

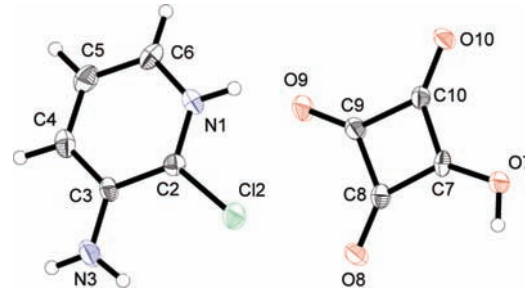

Figure 1. ORTEP diagram of **1**. Displacement ellipsoids are drawn at the 50% probability level; hydrogen atoms are drawn at arbitrary size.

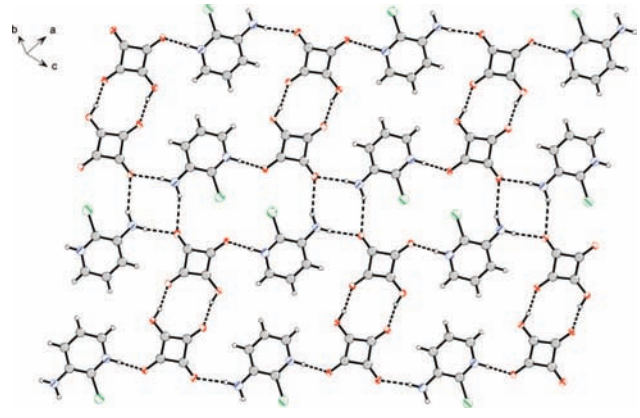

Figure 2. Hydrogen-bonding pattern in the structure of **1**. Hydrogen bonds are represented by dashed lines.

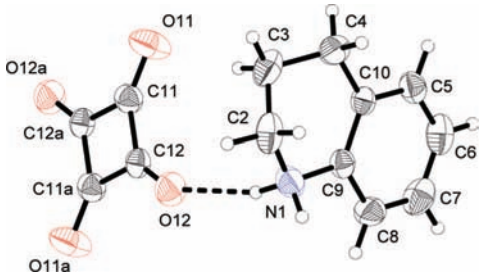

Figure 3. ORTEP diagram of **2**. Displacement ellipsoids are drawn at the 50% probability level; hydrogen atoms are drawn at arbitrary size. Symmetry related atoms are labeled with "a", and hydrogen bonds are represented by dashed lines.

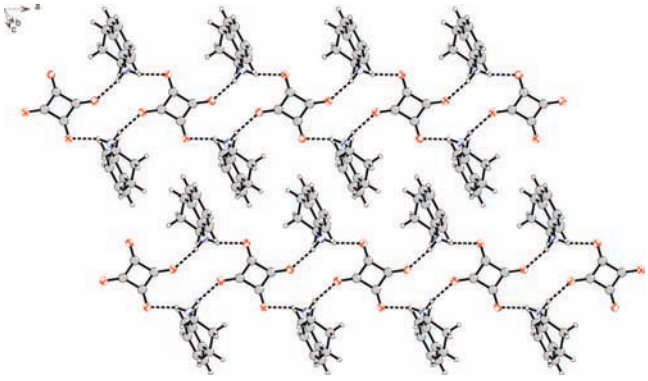

Figure 4. Hydrogen-bonding pattern in the structure of **2**. Hydrogen bonds are represented by dashed lines.

3-aminopyridine. The first one is 3-amino-2-chloropyridinium dihydrogenphosphate (CCDC code PIFJAQ[32]). It is interesting to note that in contrast to the last salt in the case of **1**, the primary NH_2-group participates in an asymmetric intermolecular hydrogen bond, leading to the assumption that the symmetric stretching vibration ν^s_{NH2} will be split into pairs of bands as a result of the FR effect.

Compound **2**, bis(1,2,3,4-tetrahydroquinolinium) squarate, also crystallizes in the triclinic in space group $P\bar{1}$ (Figure 3) but with only one formula unit per unit cell. This fact allows to us demonstrate the great advantages of the IR-LD spectroscopic tool for IR-band assignment in solids and structural elucidation of crystalline compounds. However, this is an example of a compound with an isolated squarate dianion as a structural motif (Scheme 1, **VII**). The aromatic fragment in the cation is flat, while the N1−C2−C3−C4 torsion angle in the saturated part of the cation is 61.7(2)°. The observed value is within the range of the other salts of 1,2,3,4-tetrahydroquinoline. In the hydrogen chloranilate salt (PAGXOL[33]), the value is −61.6(9)°, whereas in the 1,3,5-trinitrobenzene salt, the cation exhibits a disorder ZZZAGJ01,[34] and in the 3,5-dinitrosalicylate salt GIFNAL[35] the value is 62.0(2)°. The squarate dianion exhibits molecular D_{4h} symmetry and lies on a crystallographic center of inversion. Cations and anions are linked by intermolecular N−H···O hydrogen-bonding interactions (Figure 4). Each oxygen atom of the squarate dianion accepts one hydrogen bond from the secondary ammonium group. The N−H···O distances are 2.742(2) and 2.838(3) Å, indicating moderate hydrogen bonds. This assembly of cations and anions leads to infinite chains running along the *a* axis. The chains are interwoven by van der Waals interactions of the 1,2,3,4-tetrahydroquinolinium residues.

The bis(hydrogensquarate) dihydrate salt of 4-(aminomethyl)pyridine (**3**) is the first diprotonated form of the 4-(aminomethyl)pyridine to be investigated crystallographically. To the best

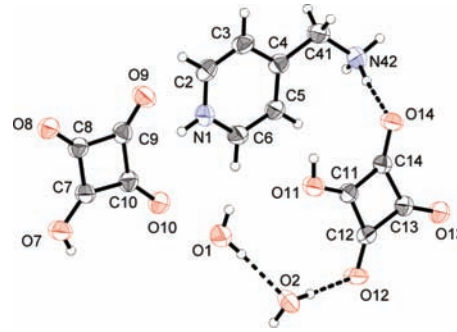

Figure 5. Asymmetric unit of **3**. Displacement ellipsoids are drawn at the 50% probability level, and hydrogen atoms are drawn at arbitrary size. Hydrogen bonds are represented by dashed lines.

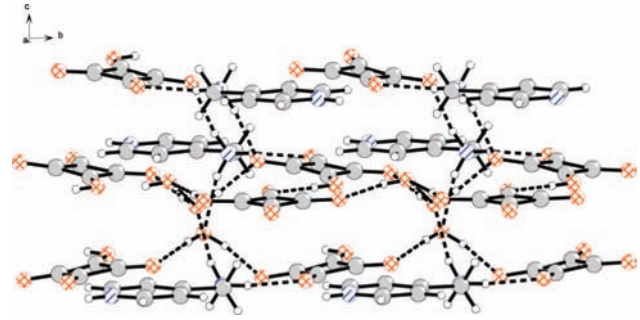

Figure 6. 3D hydrogen-bonding network of **3**. Hydrogen bonds are represented by dashed lines.

of our knowledge, only a monoprotonated form, stabilized as the hydrochloride (QANWOS[36]), is known in the literature. Compound **3** crystallizes in the monoclinic space group *P*2/*c*. The asymmetric unit comprises the 4-(ammoniummethyl)pyridinium dication, two hydrogensquarate anions, and two water molecules (Figure 5). The molecular geometry parameters of the cation and the anions lie within the typical ranges. The torsion angle of the methylammonium group out of the plane of the pyridinium ring is 5.5(2)°. The pyridinium moiety provides a moderate strong hydrogen bond to a hydrogensquarate oxygen atom with an N−H···O distance of 2.667(3) Å. The methylammonium group forms two moderate hydrogen bonds to two hydrogen squarate anions with N−H···O distances of 2.804(3) and 2.814(3) Å as well as a hydrogen bond to a solvent water molecule with an N−H···O distance of 2.806(3) Å. The two hydrogensquarate ions form a new structural motif of isolated α-joined anions with an interanionic O−H···O hydrogen-bond distance of 2.552(2) Å. This is designated as **IIb** in Scheme 1 and now reported for the first time in the literature. These pairs of anions are connected to one another by hydrogen-bonding interactions with solvent water molecules. The O−H···O distances lie in the range of 2.516(3)−2.791(2) Å. The O1−H···O2 hydrogen-bonding distance between the water molecules is 2.749(3) Å. As depicted in Figure 6, the hydrogen-bonding interactions in the crystal structure of **3** lead to a complicated 3D network structure.

Interestingly, *N*-(2-ammoniumethyl)-piperazinium hydrogensquarate squarate monohydrate (**4**) crystallizes in the monoclinic chiral space group $P2_1$. The molecular structure is shown in Figure 7. The piperazinium ring exhibits the chair conformation with the methylammonium group in axial position at N1. This is the first example of the *N*-(2-ammoniumethyl)-piperazinium trication being isolated in the present conformation in the solid state. The torsion angle of the ethylammonium group out of the mean of the plane defined by N1, N4, and C11 is about 47°. This gives rise to an axial chirality of the present

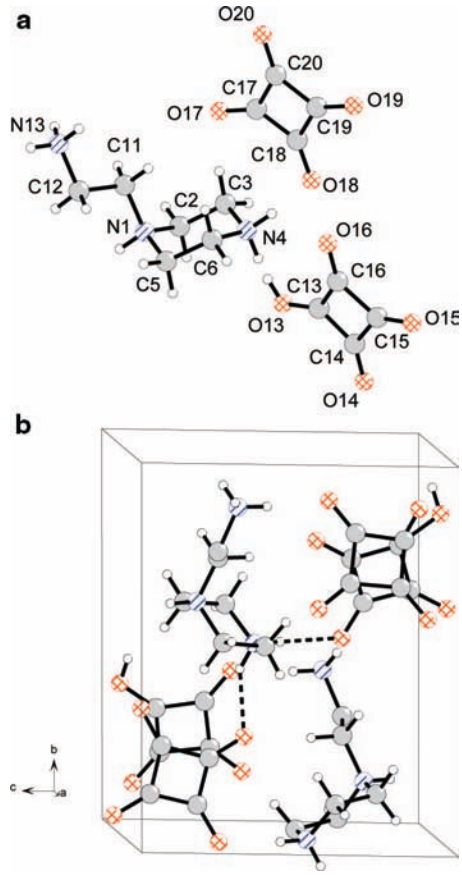

Figure 7. (a) The molecular structure of **4**. Solvent water is omitted for clarity. (b) The monoclinic unit cell of **4**. Hydrogen bonds are represented by dashed lines. Solvent water is omitted for clarity.

conformation of the cation. The squarate dianion belongs to the point group D_{4h} as in the structure of **2**. The arrangement of the molecules in the unit cell is depicted in Figure 7. The 3D hydrogen-bonding network of the structure is also complicated. The hydrogensquarate and squarate ions are joined together, forming the structural motif **IXa** in Scheme 1, by means of strong interanionic hydrogen-bonding interactions of the type O−H···O (2.511(8) Å). The *N*-(2-ammoniumethyl)-piperazinium cation forms two moderately strong hydrogen bonds to the squarate dianion via the secondary ammonium group. The N−H···O distances are 2.742(8) and 2.78(1) Å. The tertiary ammonium group provides a hydrogen bond to an oxygen atom of the hydrogensquarate ion with an N−H···O distance of 2.692(9) Å. The ethylammonium group acts as a 3-fold hydrogen-bonding donor site and forms hydrogen bonds to hydrogensquarate and squarate anions as well as to a water molecule. The corresponding N−H···O distances are in the range of 2.768(9)−2.922(9) Å.

3-Nitropyridinium hydrogensquarate monohydrate (**5**) crystallizes in the monoclinic space group *C*2/*c*. An ORTEP diagram is given in Figure 8. All molecular geometry parameters are within normal ranges. The torsion angle of the nitro group out of the plane of the pyridinium ring is ca. 17.5°.

The pyridinium moiety acts as a hydrogen-bonding donor to the hydrogensquarate ion with an N−H···O distance of 2.625(2) Å, indicating a moderate hydrogen bond. The formation of stable layered $2HSq^{-}\cdot 2H_2O$ fragments is observed (**IXb** in Scheme 1 and Figure 9). The dimers of hydrogensquarate reside on a crystallographic center of inversion. The hydrogen atom is equally disordered between O7 and its symmetry related atom

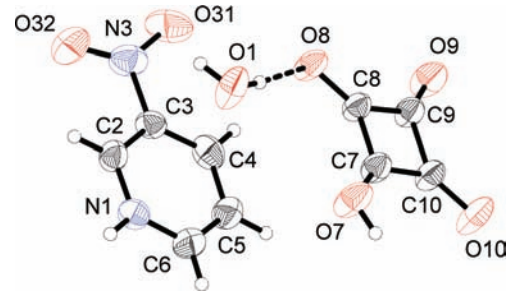

Figure 8. ORTEP diagram of **5**. Displacement ellipsoids are drawn at the 50% probability level; hydrogen atoms are drawn at arbitrary size. Hydrogen bonds are represented by dashed lines. One of the disordered parts of the hydrogen atoms is omitted for clarity.

O7A generated by inversion. The O7−H7···O7A distance is 2.449(3) Å, indicating the presence of a strong hydrogen bond. The dimer of water molecules also lies on an inversion center. One of the water hydrogen atoms is also disordered and participates in interactions of the type O1−H1B′···O1A with a distance of 2.469(4) Å. The alternative water hydrogen atom positions H1B and H8 of the hydrogensquarate anion are also half-occupied and participate in disordered hydrogen-bonding interactions O1−H1B···H8 and 01···H8−O8 with a distance of 2.631(3) Å between O1 and O8. The remaining water hydrogen atom forms a hydrogen bond to O10 of the hydrogensquarate with an O1−H1A···O10 distance of 2.618(2) Å. The C7−O7 and C8−O8 distances are 1.280(3) and 1.278(3) Å, respectively, and are equal within their standard deviation. In comparison, the C−O bond lengths of the unprotonated atoms O9 and O10 are significantly shorter with values of 1.231(3) and 1.243(3) Å, respectively. This confirms the observed positional disorder of the hydrogen atoms. This structural motif of hydrogensquarate and water molecules in **5** was recently published for the first time in the literature.[10] It is interesting to mention that as in the case of 4-cyanpyridinium hydrogensquarate monohydrate,[10] the color of the compound in the solid state is also red, thus supporting and proving additionally the phenomenon of the origin of the color in the solid state.

Conventional and Linear-Polarized IR-LD Spectra in the Solid State. In the case of **1**, our previous linear-polarized investigation[37] showed that bands at 3410 cm^{-1} (ν^{as}_{NH2}) and 3323 cm^{-1}/3202 cm^{-1} (ν^{s}_{NH2}) are observed (Figure 10). The second pairs of maxima correspond to FR splitted symmetric stretching vibrations of the ν^{s}_{NH2}, usually observed in the system, where the primary amino group participates in the asymmetric $NH_2\cdots X$ intermolecular interactions. According to the theory described above, both components will be eliminated at equal dichroic ratio, as confirmed in ref 37 for **1**. This phenomenon was observed and experimentally confirmed for the first time using the model system 4-aminopyridine.[38] In this case as well as in the case of **1**, the characteristic IR-spectroscopic regions of the discussed pairs of bands are characterized by their broad overlapped absorption bands, and for this reason to enable confirmation of the statement that the FR bands of ν^{s}_{NH2} are eliminated at equal dichroic ratio we are also presenting here the IR-LD spectroscopic characterization of 2-chloro-3-aminopyridine. The system crystallized in the monoclinic space group $P2_1/n$ and $Z = 4$ (YELSEO CCDC code).[39] The IR-LD spectra of this compound are characterized by well-defined IR maxima and the excellent degree of orientation shown in Figure 3, using the criteria in refs 29−32. As can be seen, the elimination of the bands at 3451 cm^{-1} leads to the disappearance of the series of benzene in-plane IR bands at 1563, 1272, 1141, and 688 cm^{-1} (Figure 10, part (3)). In all cases, the elimination

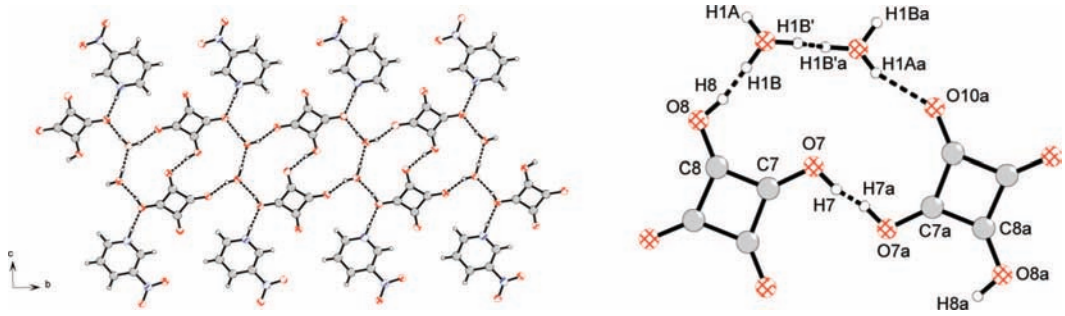

Figure 9. The crystal structure of **5** viewed along the *a* axis showing the hydrogen-bonding pattern. Hydrogen bonds are represented by dashed lines. One of the disordered parts of the hydrogen atoms is omitted for clarity.

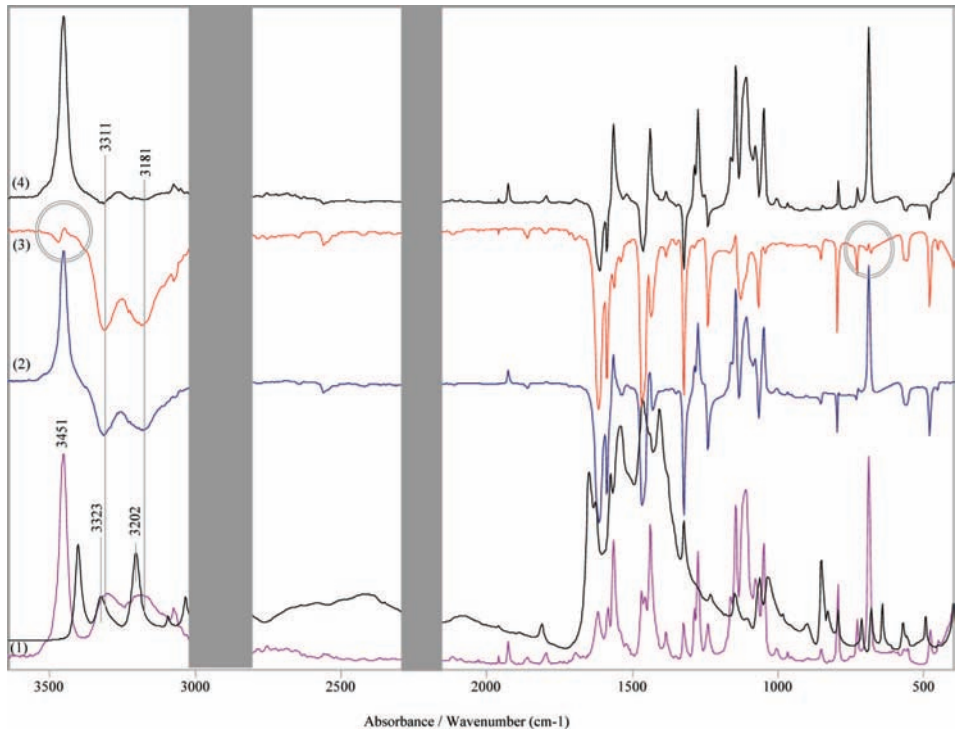

Figure 10. Solid-state nonpolarized IR (1), difference IR-LD (2), and reduced IR-LD spectra in nematic host of 2-chloro-3-aminopyridine after elimination of the bands at 3451 cm^{-1} (3) and 3311 cm^{-1} (4); IR spectrum of **1** in nematic mesophase. Grey rectangles show the self-absorption band of the nematic mesophase.

leads to a so-called "inflex point" as a result of the multiple character of these maxima or DS effect. This phenomenon has been mentioned in refs 40, 41. The multicomponent IR band in this case is split according to the number of the molecules in the unit cell in the components with different intensities (see above and ref 32), and these components have different polarization if the molecules are oriented in a different way. The elimination of the components of the band at 688 cm^{-1} at different dichroic ratio is observed. As in the case of **1**, the IR-spectroscopic data for the neutral 2-chloro-3-aminopyridine are confirmed by the crystallographic data. According to ref 39, the unit cell of 2-chloro-3-aminopyridine contains $Z = 4$, and the molecules are joined into infinite chains by means of asymmetric moderate intermolecular HNH···N intermolecular interactions (3.088 Å). The different molecules are mutually oriented at an angle of 61.9(1)° between the aromatic fragments (Figure S1).

The fact that asymmetric hydrogen bonding of the HNH···N type is observed in the solid state leads to an FR splitting of the ν^{s}_{NH2} band into pairs, eliminating at equal dichroic ratio. As can be seen, the bands at 3311 and 3181 cm^{-1} are eliminated simultaneously (Figure 10, part (4)).

In contrast to the corresponding hydrogensquarate salt (**1**) and the simpler model system 2-chloro-3-aminopyridine, the spectroscopic patern of **2** is characterized by a broad absorption band within the whole 3200−2000 cm^{-1} region (Figure S2) belonging to asymmetric and symmetric stretching vibrations (ν^{as}_{N+H2}, ν^{s}_{N+H2}) of the protonated secondary amine. The observed broad character of the bands is typical for the amino acids and peptides and can be attributed to the FR effect as well. The corresponding submaxima are eliminated at an equal dichroic ratio. The same effect has been proposed for the carboxylic acid dimmers (see Supporting Information). The strong overlapping effect observed in this compound makes it difficult to interpret the IR bands in the whole 4000−850 cm^{-1} region at a significant level, and only the bands within 850−400 cm^{-1} were therefore processed by the reducing difference method. This example is useful for demonstrating the application of the last approach for interpretating the IR spectra of crystalline samples when the unit cell of **2** contains $Z = 1$. As can be seen, the elimination of the band at 755 cm^{-1} leads to its total disappearance.

Similar to **1**, the IR spectra of **3**−**5** (Figure 11) are characterized by broad absorption bands within the 2100−2000 cm^{-1}

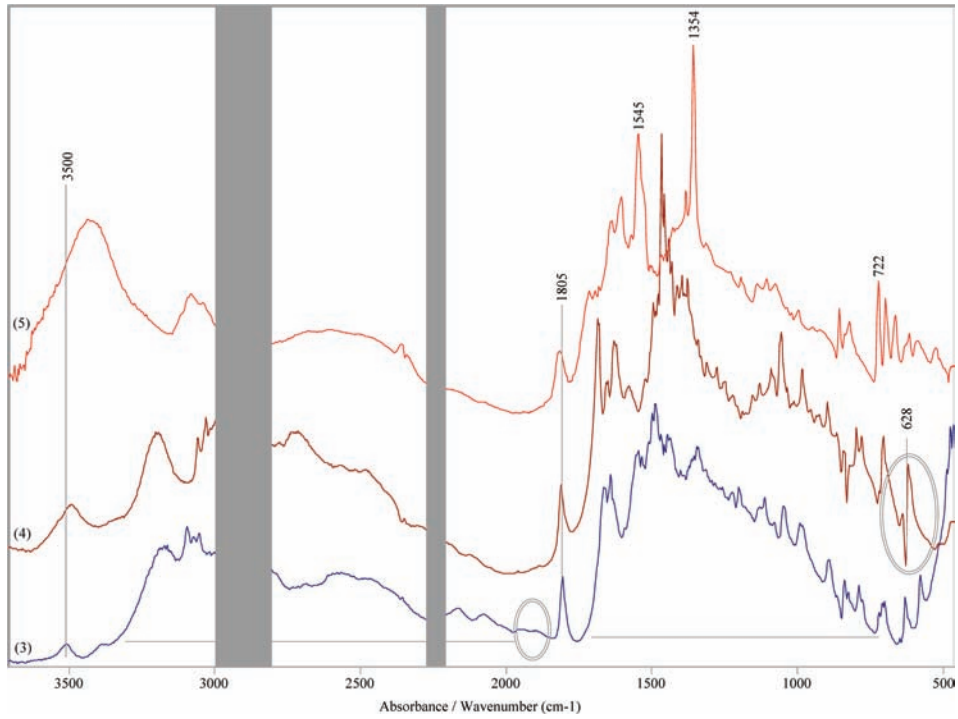

Figure 11. IR spectra of compounds **3**−**5** in the solid state in nematic liquid crystal host.

region corresponding to ν_{OH} stretching vibrations of the OH group in the hydrogensquarate anions overlapped with corresponding stretching modes of the different protonated amino groups. These broad bands are characterized by series of submaxima with different polarizations (obtained by their difference IR-LD spectra), thereby indicating an FD effect. The bands at about 3500 cm^{-1} belong to the solvent water molecules. The discussed broadband is a typical spectroscopic curve for the hydrogensquarates, leading to difficulties in interpreting other IR bands within this region. In some hydrogensquarates, the lowest frequency submaxima are obtained at about 1900 cm^{-1},[16] for example, Figure 11. More characteristic for hydrogensquarates is the appearance of the band about 1800 cm^{-1} belonging to symmetric stretching ($\nu^{s}_{CO(HSq)}$) vibrations of HSq^{-}. This maximum can be used for studying of the DS effect depending on the number of the molecules in the unit cell and their mutual orientation. For compounds **3** and **4**, the elimination of this band leads to an "inflex point" picture, while in **5** total disappearance of the band occurs, like the effect in **2**. The observations are confirmed by our crystallographic data for the orientation of the molecules in the unit cells of **3**−**5**, respectively (see above). The hydrogensquarates are characterized as well by the broad absorption band within the 1700−800 cm^{-1} region, which is also the result of the FD effect. These bands are usually of strong intensity, and only in the case of **3**, where the cation contains an NO_2-group, are stronger IR bands belonging to ν^{as}_{NO2} and ν^{s}_{NO2} at 1545 and 1354 cm^{-1} observed. The IR characteristics of these compounds can be successfully assigned using the region 850−400 cm^{-1}, but attention must be paid to the Evans' hole effect (Figure 11).

The discussed regions and possibilities for the interpretation of the IR spectra as well as the corresponding limitations are common for all of the hydrogensquarates, independent of the structural motifs of these compounds. In the course of our systematic study, we have compared, for example, the corresponding characteristics of the hydrogensquarate salt of 1,10-phenanthroline (structural motif **Ib**)[42] with those of cyclohexylamonium hydrogensquarate monohydrate, characterizing the α-chain (**IIa**),[43] L-argininium and L-serinium hydrogensquarates,[44,45] the **IIIa** and **IIIb** structural motifs, $H_2Sq \cdot HSq^{-} \cdot 2H_2O$ (**IVa**),[16] the nonplanar tetrameric motif of guanidinium hydrogensquarate (**IVb**),[46] the tetrameric motif (**IVc**) or isolated hydrogensquarate anion (**VIII**) in the L-lysinium salts,[26] as well as the layered motif (**IXb**),[10] leading to the observation of the red color in the last compound in the solid state (Scheme 1).

Acknowledgment. B.B.K. wishes to thank the Alexander von Humboldt Foundation for a Fellowship, and T.K. thanks the DAAD for a grant within the priority program "Stability Pact South-Eastern Europe" and the Alexander von Humboldt Foundation.

Supporting Information Available: Crystallographic data for the structural analysis have been deposited with the Cambridge Crystallographic Data Centre, CCDC 711322-711326. Copies of this information may be obtained from the Director, CCDC, 12 Union Road, Cambridge CB2 1EZ, UK (fax, +44 1223 336 033; e-mail, deposit@ccdc.cam.ac.uk or http://www.ccdc.cam.ac.uk). This material is available free of charge via the Internet at http://pubs.acs.org.

References and Notes

(1) Davydov, A. S. *Theory of Molecular Excitons*; McGraw Hill: New York, 1968.
(2) Davydov, A. S. *Theory of Molecular Excitons*; Nauka: Moscow, 1962.
(3) Winston, H. *J. Chem. Phys.* **1951**, *19*, 156.
(4) McClure, D. S. *J. Chem. Phys.* **1954**, *22*, 1256.
(5) Lisitsa, M. P.; Ralko, N. E.; Yaremko, A. M. *Phys. Lett. A* **1972**, *40*, 329.
(6) Lisitsa, M. P.; Ralko, N. E.; Yaremko, A. M. *Phys. Lett. A* **1974**, *48*, 241.
(7) Lisitsa, M. P.; Ralko, N. E.; Yaremko, A. M. *J. Mol. Cryst. Liq. Cryst.* **1974**, *28*, 161.
(8) Lisitsa, M. P.; Yaremko, A. M. *J. Mol. Cryst. Liq. Cryst.* **1972**, *18*, 297.
(9) Lisitsa, M. P.; Yaremko, A. M. *J. Mol. Cryst. Liq. Cryst.* **1972**, *19*, 1.

(10) Koleva, B.; Kolev, T.; Seidel, R.; Mayer-Figge, H.; Spiteller, M.; Sheldrick, W. *J. Phys. Chem.* **2008**, *112A*, 2899.
(11) Kolev, T.; Zareva, S.; Mayer-Figge, H.; Spiteller, M.; Sheldrick, W.; Koleva, B. *Amino Acids*, in press.
(12) Kolev, T.; Koleva, B. B.; Emgenbroich, M.; Spiteller, M.; Sheldrick, W. S.; Mayer-Figge, H. *Struct. Chem.* **2006**, *17*, 631.
(13) Kolev, T.; Ivanova, B. B.; Bakalska, R. *J. Mol. Struct.* **2006**, *794*, 138.
(14) Kolev, T.; Seidel, R. W.; Koleva, B. B.; Spiteller, M.; Mayer-Figge, H.; Sheldrick, W. S. *Struct. Chem.* **2008**, *19*, 101.
(15) Koleva, B. B.; Kolev, T.; Seidel, R. W.; Tsanev, Ts.; Mayer-Figge, H.; Spiteller, M.; Sheldrick, W. S. *Spectrochim. Acta, Part A*, in press, doi: 10.1016/j.saa.2008.01.033.
(16) Kolev, T.; Koleva, B.; Seidel, R.; Spiteller, M.; Sheldrick, W. *Acta Crystallogr.* **2007**, *E63*, o4852.
(17) Gilli, G.; Bertolasi, V.; Gilli, P.; Ferretti, V. *Acta Crystallogr.* **2001**, *B57*, 859.
(18) Karle, I.; Ranganathan, D.; Haridas, V. *J. Am. Chem. Soc.* **1996**, *118*, 7128.
(19) Yesilel, O. Z. *J. Mol. Struct.* **2008**, *874*, 151.
(20) Yesilel, O. Z.; Pasaoglu, H.; Yilanve, O.; Büyükgüngör, O. *Z. Naturforsch.* **2007**, *62b*, 823.
(21) Yesilel, O.; Odabasoglu, M.; Ölmez, H.; Büyükgüngör, O. *Z. Naturforsch.* **2006**, *61b*, 1243.
(22) Uçar, I.; Bulut, A.; Yesilel, O. Z.; Büyükgüngör, O. *Acta Crystallogr.* **2004**, *C60*, o585.
(23) Bulut, A.; Yesilel, O.; Dege, N.; Içbudak, H.; Ölmez, H.; Büyükgüngör, O. *Acta Crystallogr.* **2003**, *C59*, o727.
(24) Kolev, T.; Seidel, R. W.; Spiteller, M.; Mayer-Figge, H.; Sheldrick, W. S.; Koleva, B. B. *J. Mol. Struct.*, in press.
(25) Blessing, R. H. *Acta Crystallogr.* **1995**, *A51*, 33.
(26) Spek, A. L. *J. Appl. Crystallogr.* **2003**, *36*, 7.
(27) Sheldrick, G. M. *Acta Crystallogr.* **2008**, *A64*, 112.
(28) Ivanova, B. B.; Arnaudov, M. G.; Bontchev, P. R. *Spectrochim. Acta* **2004**, *60A*, 855.
(29) Ivanova, B. B.; Tsalev, D. L.; Arnaudov, M. G. *Talanta* **2006**, *69*, 822.
(30) Ivanova, B. B.; Simeonov, V. D.; Arnaudov, M.; Tsalev, D. *Spectrochim. Acta* **2007**, *67A*, 66.
(31) Koleva, B.; Kolev, T.; Simeonov, V.; Spassov, T.; Spiteller, M. *J. Inclusion Phenom.* **2008**, *61*, 319.
(32) Hamed, K.; Samah, A.; Mohamed, R. *Acta Crystallogr.* **2007**, *63E*, o2896.
(33) Ispida, H. *Acta Crystallogr.* **2004**, *60E*, o1674.
(34) Smith, G.; Wermuth, U. D.; White, J. M. *Acta Crystallogr.* **2002**, *58E*, o1130.
(35) Smith, G.; Wermuth, U. D.; Healy, P. C.; White, J. M. *Aust. J. Chem.* **2007**, *60*, 264.
(36) de Vries, E. J. C.; Oliver, C. L.; Lloyd, G. O. *Acta Crystallogr.* **2005**, *61E*, 01577.
(37) Kolev, T.; Tsanev, T. *Bulg. Chem. Commun.*, in press.
(38) Arnaudov, M. G.; Ivanova, B. B.; Dinkov, Sh. G. *Vib. Spectrosc.* **2005**, *37*, 145.
(39) Saha, B. K.; Nangia, A.; Nicoud, J.-F. *Cryst. Growth Des.* **2006**, *6*, 1278.
(40) Arnaudov, M. *Bulg. Chem. Commun.* **2005**, *37*, 230.
(41) Arnaudov, M.; Ivanova, B. *Bulg. Chem. Commun.* **2005**, *37*, 283.
(42) Kolev, Ts.; Koleva, B.; Seidel, R. W.; Mayer-Figge, H.; Spiteller, M.; Sheldrick, W. S. *Spectrochim. Acta, Part A*, in press.
(43) Kolev, T.; Koleva, B.; Seidel, R.; Spitreller, M.; Sheldrick, W. *Acta Crystallogr.* **2007**, *E63*, o4852.
(44) Angelova, O.; Velikova, V.; Kolev, T.; Radomirska, V. *Acta Crystallogr.* **1996**, *C52*, 3252.
(45) Kolev, T.; Stahl, R.; Preut, H.; Bleckmann, P.; Radomirska, V. *Z. Kristallogr.* **1998**, *213*, 169.
(46) Kolev, T.; Preut, H.; Bleckmann, P.; Bleckmann, P.; Radomirska, V. *Acta Crystallogr.* **1997**, *C53*, 805.

JP8106233